USCAP

www.nature.com/labinvest

ARTICLE

Check for updates

Smoothened (SMO) regulates insulin-like growth factor 1 receptor (IGF1R) levels and protein kinase B (AKT) localization and signaling

Nitin K. Agarwal[1], Chae-Hwa Kim[2], Kranthi Kunkalla[2], Amineh Vaghefi[2], Sandra Sanchez[2], Samantha Manuel[3], Daniel Bilbao[4], Francisco Vega[1,6]✉ and Ralf Landgraf[3,4,5,6]✉

The oncoprotein Smoothened (SMO), a Frizzled-class-G-protein-coupled receptor, is the central transducer of hedgehog (Hh) signaling. While canonical SMO signaling is best understood in the context of cilia, evidence suggests that SMO has other functions in cancer biology that are unrelated to canonical Hh signaling. Herein, we provided evidence that elevated levels of human SMO show a strong correlation with elevated levels of insulin-like growth factor 1 receptor (IGF1R) and reduced survival in diffuse large B-cell lymphoma (DLBCL). As an integral component of raft microdomains, SMO plays a fundamental role in maintaining the levels of IGF1R in lymphoma and breast cancer cells as well IGF1R-associated activation of protein kinase B (AKT). Silencing of *SMO* increases lysosomal degradation and favors a localization of IGF1R to late endosomal compartments instead of early endosomal compartments from which much of the receptor would normally recycle. In addition, loss of SMO interferes with the lipid raft localization and retention of the remaining IGF1R and AKT, thereby disrupting the primary signaling context for IGF1R/AKT. This activity of SMO is independent of its canonical signaling and represents a novel and clinically relevant contribution to signaling by the highly oncogenic IGF1R/AKT signaling axis.

Laboratory Investigation (2022) 102:401–410; https://doi.org/10.1038/s41374-021-00702-6

INTRODUCTION

The IGF signaling axis has been recognized as an important contributor to both carcinogenesis and the emergence of drug resistance across a wide array of cancers[1–3]. As a receptor tyrosine kinase, much of the canonical signaling downstream of IGF1R includes elements found for other receptor tyrosine kinases (RTKs). However, like several other RTKs, it has also become clear that IGF1R signaling exhibits features that are more reminiscent of G-protein coupled receptor (GPCR) signaling[4]. Its internalization can proceed through the more conventional interaction with adapters such as growth factor receptor-bound protein 10 (GRB10)[5], but it can also utilize b-arrestin1 to facilitate rapid internalization and signaling through the mitogen-activated protein kinase (ERK) pathway[6]. In addition, IGF1R displays SUMO-dependent nuclear localization that contributes to proliferation in cancer cells[7–9]. While IGF1R resembles other RTKs in its ability to stimulate phosphoinositide-3-kinase (PI3K)/AKT and MAPK signaling, the regulation of both signaling events displays very pronounced divergence in terms of its requirements for sustained activation or ubiquitination to signal into both pathways[10]. Central to all these functional aspects is the regulation of its localization, internalization, turnover, and processing, which orchestrates the multiple signaling options available to IGF1R[11].

Smoothened (SMO) is a seven-transmembrane frizzled-class G-protein-coupled receptor that is best known for its ability to transduce the signal that is generated when ligands of the hedgehog family bind to their immediate target, patched (PTCH1). This binding releases the inhibition that PTCH1 exerts on SMO[12]. Activating mutations in SMO or the loss of its negative regulator PTCH1 are oncogenic events[13]. SMO contains an N-terminal extracellular segment with a cysteine-rich domain (CRD), a heptahelical transmembrane domain (TMD), and a C-terminal intracellular segment[14]. Conventional SMO signaling in vertebrates functions in many differentiated cells and localizes to cilia, a highly specialized surface organelle in developmental signaling[15]. Cilia are dissembled during mitosis and loss of cilia assembly has a mild phenotype compared to the loss of SMO signaling components[16], suggesting that SMO functions go beyond its role in cilia activity. Moreover, previous studies in Drosophila cells that lack cilia, except for olfactory sensory neurons[17], suggest that SMO is also broadly localized to lipid rafts[18,19]. Beyond Hh-initiated and PTCH1 controlled signal transduction, SMO is directly activated by oxysterols, and recent studies suggest that cholesterol, a ubiquitous component of lipid rafts, is the primary ligand of SMO. Indeed cholesterol-binding results in a conformational change in SMO that enables the downstream events of canonical

[1]Division of Hematopathology, The University of Texas M D Anderson Cancer Center, Houston, TX, USA. [2]Division of Hematopathology, Sylvester Comprehensive Cancer Center, University of Miami, Miami, FL, USA. [3]Sheila and David Fuente Graduate Program in Cancer Biology, Miller School of Medicine, University of Miami, Miami, FL, USA. [4]Sylvester Comprehensive Cancer Center, University of Miami, Miami, FL, USA. [5]Department of Biochemistry and Molecular Biology, Miller School of Medicine, University of Miami, Miami, FL, USA. [6]These authors contributed equally: Francisco Vega, Ralf Landgraf. ✉email: fvega@mdanderson.org; RLandgraf@med.miami.edu

Received: 6 April 2021 Revised: 14 October 2021 Accepted: 14 October 2021
Published online: 10 December 2021

Hh signaling[14,19], but the role of SMO in cancer, independent of its canonical Hh signaling function, still remains poorly understood.

Critical contributions to cancer cell survival by SMO and IGF1R converge at the level of PI3K/AKT signaling. Constitutive PI3K/AKT is an important contributor to cellular stress adaptation in many cancers, including diffuse large B-cell lymphoma (DLBCL)[20–22]. PI3K/AKT signaling provides critical survival signals downstream of the B-cell receptor and other membrane-bound receptors that respond to various cytokines and growth factors[23,24]. In a subset of DLBCL, PI3K/AKT activation is constitutively enhanced by the loss of phosphatase and tensin homolog (PTEN)[21,22].

We have previously shown that one way by which SMO contributes to the enhancement of AKT signaling through an additional, noncanonical mechanism, is the recruitment of ubiquitinating and deubiquitinating enzymes that shift the balance of different types of ubiquitination branching, resulting in increased levels of activated pAKT[17].

On the level of transcriptional regulation and canonical signaling, IGF1-induced activation of AKT potentiates GLI transcriptional activity upon stimulation with sonic hedgehog (Shh)[25]. Stimulation by Shh and IGF1 synergizes in somite myogenesis[26], and IGF1-dependent activation of AKT and MAPK in myocytes is suppressed by the SMO inhibitor, cyclopamine[27]. However, given the ability of SMO to regulate the stability of membrane-localized and activated AKT by noncanonical means at a post-translational level, we wanted to know whether its influence on the stability of critical oncogenic membrane signaling components extends further, including receptors, such as IGF1R, that prominently signal into the AKT pathway. Indeed, we found that IGF1R and SMO show a strong correlation in DLBCL at the protein level, and levels of IGF1R protein are substantially reduced upon loss of SMO by means that do not depend on canonical signaling. Further investigation of this regulation shows that loss of SMO reduces IGF1R levels by favoring lysosomal degradation over recycling and disrupts the signaling context of the remaining pool of IGF1R in a way that largely disables AKT signaling.

MATERIALS AND METHODS

Cell lines and cell viability assays

SUDHL4 cells were purchased from DSMZ (Braunschweig, Germany). HBL1 cells were kindly provided by Dr. Samaniego (Department of Lymphoma and Myeloma, MD Anderson Cancer Center, Houston, TX) and Dr. Schatz (Department of Medicine, Sylvester Comprehensive Cancer Center, University of Miami), respectively. MDA-MB-231 and SMO$^{-/-}$ mouse embryonic fibroblast (MEF) cells were a gift from Dr. Rosenblatt (Department of Medicine, Sylvester Comprehensive Cancer Center, University of Miami) and Dr. James K. Chen (Department of Chemical and Systems Biology, Stanford University School of Medicine), respectively. DLBCL and MDA-MB-231 cell lines were maintained at 37 °C in RPMI 1640 (ATCC) supplemented with 10% heat-inactivated fetal bovine serum (FBS) (Sigma-Aldrich, MO) and 0.2% MycoZap Plus-CL (Lonza, Switzerland) in a humidified atmosphere containing 5% CO_2. When mentioned, cells were either stimulated with growth factors (IGF, EGF, VEGF, or FGF) or treated with Bafilomycin (BAF, 100 nM) for the indicated periods and at the indicated concentrations.

Immunohistochemical studies

We used a tissue microarray (TMA) with reactive lymph nodes and DLBCL tumors ($n = 60$) collected from formalin-fixed, paraffin-embedded archival tumor specimens. Tissue specimens were collected from Sylvester Comprehensive Cancer Center, University of Miami as approved by the institutional review board committee. The study was conducted in accordance with the declaration of Helsinki. According to the expression of CD10, BCL-6, and MUM-1 (30% cutoff), cases were classified as either GC or non-GC (ABC) type using the Hans algorithm[28]. Immunohistochemistry studies were performed as described previously[29] using prediluted primary antibodies for CD10, BCL-6, MUM-1 (Leica Biosystems, IL), and SMO (ab72130; 1:2000; Abcam, MA).

Plasmids and RNA interference

Recombinant human SMO, and part of the cytomegalovirus (CMV) promoter, was cloned into the Nhel and Agel sites of the mammalian mCherry-C1 expression vector to create a SMO-mCherry C-terminal fusion protein. Lentiviral human SMO shRNA was purchased from Sigma Mission shRNA (Sigma-Aldrich, MO). Transfections and lentiviral particle formation, and infections were performed as described previously[30].

Cell lysates and immunoblotting

Cells were rinsed with ice-cold phosphate-buffered saline (PBS) and lysed in RIPA buffer containing 20 mM Tris-HCl (pH 7.5), 150 mM NaCl, 1 mM EDTA, 1% NP-40, 1% sodium deoxycholate, 2.5 mM sodium pyrophosphate, 1 mM beta-glycerophosphate, 1 mM sodium orthovanadate, and complete protease inhibitor (Roche Applied Science). The cell lysates were incubated for 20 min at 4 °C and processed for SDS page and immunoblotting. The antibodies SMO (ab72130; 1:1000; Abcam), IGF1R, EGFR, pAKT (S473), pAKT (T308), AKT (1:1000; Cell Signaling), actin-HRP (1:10,000; Sigma-Aldrich), Flotillin, Caveolin-1 and Transferrin receptor (TF-R, 1:1000; Santa Cruz, TX) were used overnight at 4 °C.

Immunofluorescence analysis

Immunofluorescence staining of CD59, TF-R, and SMO proteins was performed on live HBL1 cells. To enhance rapid clustering, primary antibodies CD59 (Invitrogen, CA), transferrin receptor (TF-R, Santa Cruz, TX), and SMO (Abcam, MA) were first prebound to their respective secondary antibodies (Millipore, MA) for 1 h. Cells were stained with the primary/secondary conjugates for 30 min at room temperature and subsequently fixed in 4% paraformaldehyde at room temperature for 10 min, washed with PBS, and stained with DAPI. Confocal imaging was performed using a Leica microscope with a ×63 objective.

Cholera toxin-B (CTB) immunofluorescence staining was performed as described[31]. MDA-MB-231 cells that stably overexpress SMO were cultured overnight in six-well plates in fresh RPMI medium. The next day, cells were washed with PBS and resuspended in 100 µl. Cells were subsequently stained with 2 µl CTB-FITC (2.0 µg/ml) at room temperature for 1 h. Cells were fixed in 4% paraformaldehyde at room temperature for 15 min, washed with PBS twice, and incubated overnight at 4 °C with rabbit antibodies against IGF1R, or mouse antibodies against RAS-associated protein 5 (RAB5) or RAS-associated protein 7 (RAB7) (Cell Signaling, MA). Samples were imaged by confocal microscopy.

Lipid raft fractionations

MDA-MB-231 cells were fractionated following a detergent-free method adapted from Prior et al.[32]. Briefly, 100 million cells were washed in PBS, centrifuged, and resuspended in 0.5 M Na_2CO_3 solution. After homogenization through 30 & 23-gauges needles and sonication, lysates were mixed 1:1 with 90% sucrose in MES-buffered saline (MBS; 25 mM MES, pH 6.5, 150 mM NaCl). We overlaid 1 ml of 45% sucrose/lysate sequentially with 1.2 ml of 35% sucrose, 1 ml of 30% sucrose, 1 ml of 25% sucrose, and 1 ml of 5% sucrose and centrifuged the gradient in a Beckman SW-55 rotor for 16 h at 48,000 rpm at 4 °C. Ten 0.5-ml fractions were collected from the top of the gradient and subjected to Immunoblotting.

RNA extraction and quantitative real-time PCR analysis

Quantitative (q) real-time PCR analyses were performed as described previously[33]. Primers used for q-PCR analyses were purchased from Applied Biosystems (MA). Each target was amplified in duplicate, and data analyses were done using the 2−ΔΔCT method.

Statistical analysis

Survival curves of DLBCL patients with low and high expression of SMO were stratified using microarray data available in a public repository (GSE10846). Log2 median-centered intensities of SMO (probe 218629_at) in 414 DLBCL cases were obtained by using Oncomine version 4.5 (www.oncomine.org). High and low SMO gene expression (mRNA levels) was determined as follow: high expression levels were considered those above M + 1 SD and low levels were those below M-1SD with M being the mean (M) and SD the standard deviation. The patient overall survival of the two groups was calculated. The Kaplan–Meier survival curve of SMO gene expression data was retrieved from a public repository (GSE10846; $n = 414$) using gene expression Oncomine v4.5 software.

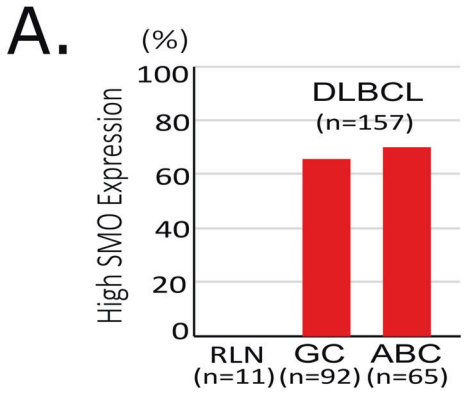

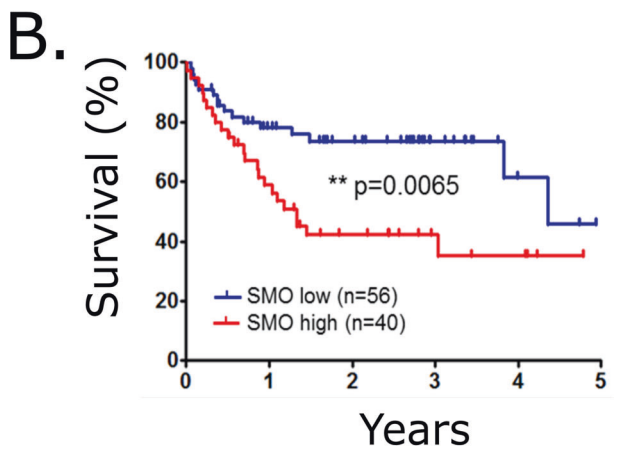

C.

		SMO		Total
		Weak Positive	Strong Positive	
IGF1R	Weak Positive	5 (9.25%)	4 (7.4%)	9
	Strong Positive	6 (11.1%)	39 (72.2%)	45
Total		11	43	54

Fig. 1 Elevated protein levels of SMO correlate with high IGF1R and poor survival in DLBCL. A Immunohistochemistry of SMO was performed in DLBCL (ACB or GC) tissue sections ($n = 157$). Quantification of the SMO percentages of positive cells in DLBCL tumor sections was scored using the following system: Negative = 0–24%; positive = 25–100%. **B** Kaplan–Meier survival curve of *SMO* gene expression data was retrieved from a public repository (GSE10846; $n = 414$) using gene expression Oncomine v4.5 software. **C** Correlation of SMO and IGF1R levels by immunohistochemistry in DLBCL tissue microarray sections ($n = 54$).

RESULTS

Elevated protein levels of SMO correlate with high IGF1R and poor survival in DLBCL

We had recently reported a role of SMO in the stabilization of TNF receptor-associated factor 6 (TRAF6) and subsequent stabilization of AKT that did not involve canonical signaling by SMO but rather required elevated levels of SMO to act in a scaffold-like fashion[34]. Given the role of IGF1R in DLBCL in general and AKT signaling in particular, we wanted to know if a clinically relevant correlation also existed for SMO and IGF1R on a protein level. We, therefore, evaluated the extent of coexpression of the SMO and IGF1R protein by immunohistochemistry in DLBCL patient samples. We first validated the specificity of the SMO antibody staining using an SMO negative, reactive lymph node and SMO positive prostate cancer section (Supplementary Fig. 1). While high levels of IGF1R have been established in DLBCL[35], less is known about SMO expression. Compared to reactive lymph node as a negative control, DLBCL samples displayed elevated levels of SMO, and quantification of 157 DLBCL tumors collected from patient samples showed high SMO protein levels, both in germinal center (GC) and activated B-cell (ABC) subtypes (Fig. 1A). Clinically, high levels of SMO show a strong correlation with decreased survival (Fig. 1B). When we evaluated the same DLBCL samples for the levels of both IGF1R and SMO, we found a strong correlation between both (Fig. 1C). These data suggest not only that SMO itself is a potential oncogenic contributor in DLBCL but they also point towards a potential link between the protein levels of IGF1R and SMO.

SMO enhances IGF1R-mediated phosphorylation of AKT

The strong correlation levels between IGF1R and SMO, the negative correlation of high SMO levels with survival, and the important role of AKT as a downstream target of IGF1R signaling in tumorigenesis and drug resistance, raises the question of whether simultaneous high levels of both receptors synergize directly at the level of AKT activation, beyond the established synergy on a transcriptional level. To evaluate the potential role of SMO in the growth factor-initiated activation of AKT, we first tested the impact of SMO deletion on receptor stimulation using wild-type or $SMO^{-/-}$ mouse embryonic fibroblasts (MEF $SMO^{+/+}$ and MEF $SMO^{-/-}$) (Fig. 2A, B).

When cells grown under reduced serum conditions (2%) are stimulated with recombinant human IGF1, MEF cells show increased AKT phosphorylation at S473 and T308 (Fig. 2A), and this activation is markedly diminished in MEF cells lacking SMO (MEF $SMO^{-/-}$). However, the pronounced defect in AKT activation does not occur at a significant level for ERK1/2, where both phosphorylation and protein levels show largely the same response pattern with or without SMO depletion. As an unrelated receptor control, IL6-dependent activation of AKT is not impacted (Fig. 2B). When the DLBCL cell line HBL1 (ABC-type) is stimulated with IGF1, the activation of AKT is also diminished upon shRNA-based knockdown of SMO (Fig. 2C). Both the levels and activation of IRS1, an integral part of IGF1R-dependent activation of AKT, are greatly diminished (Fig. 2C). The analysis of IGF1R levels shows a pronounced decrease in receptor levels, although residual levels differ in various cellular settings (Figs. 3A, D and 5E). As was the case for MEF cells lacking SMO, no significant change was observed for ERK1/2 activation, suggesting that IGF1R levels have not only changed quantitatively but the signaling context and outcomes of the remaining IGF1R receptors have changed as a result of losing SMO. Notably, in unstimulated shSMO cells a disproportional level of basal phosphorylation occurs on Tyr1135 (1165). This position does not report on the phosphorylation state of the tail region of the receptor, needed for adapter recruitment, but reports on the activation loop and catalytic state. While phosphorylation and ubiquitination of the C-terminal tail of IGF1R is needed for MAPK signaling, the activation of this pathway needs only very short-lived IGF1R activation to induce MAPK signaling while AKT signaling requires sustained activation. In fact, IGF1R activation starting at 1 min, peaking at 5 and returning to low levels by 10 min are sufficient to trigger MAPK signaling[10]. The loss of activation loop phosphorylation is therefore consistent with a loss of AKT signaling but unimpeded signaling by MAPK.

To further validate the role of SMO in AKT signaling across model systems, we evaluated the impact of shSMO in MDA-MB-231, a triple-negative breast cancer cell line (Fig. 2D). As was the case for MEF and HBL1 cells, a substantial knockdown of SMO reduced AKT activation, although the impact of SMO depletion manifests itself primarily for the activation at Thr308. AKT phosphorylation at T308

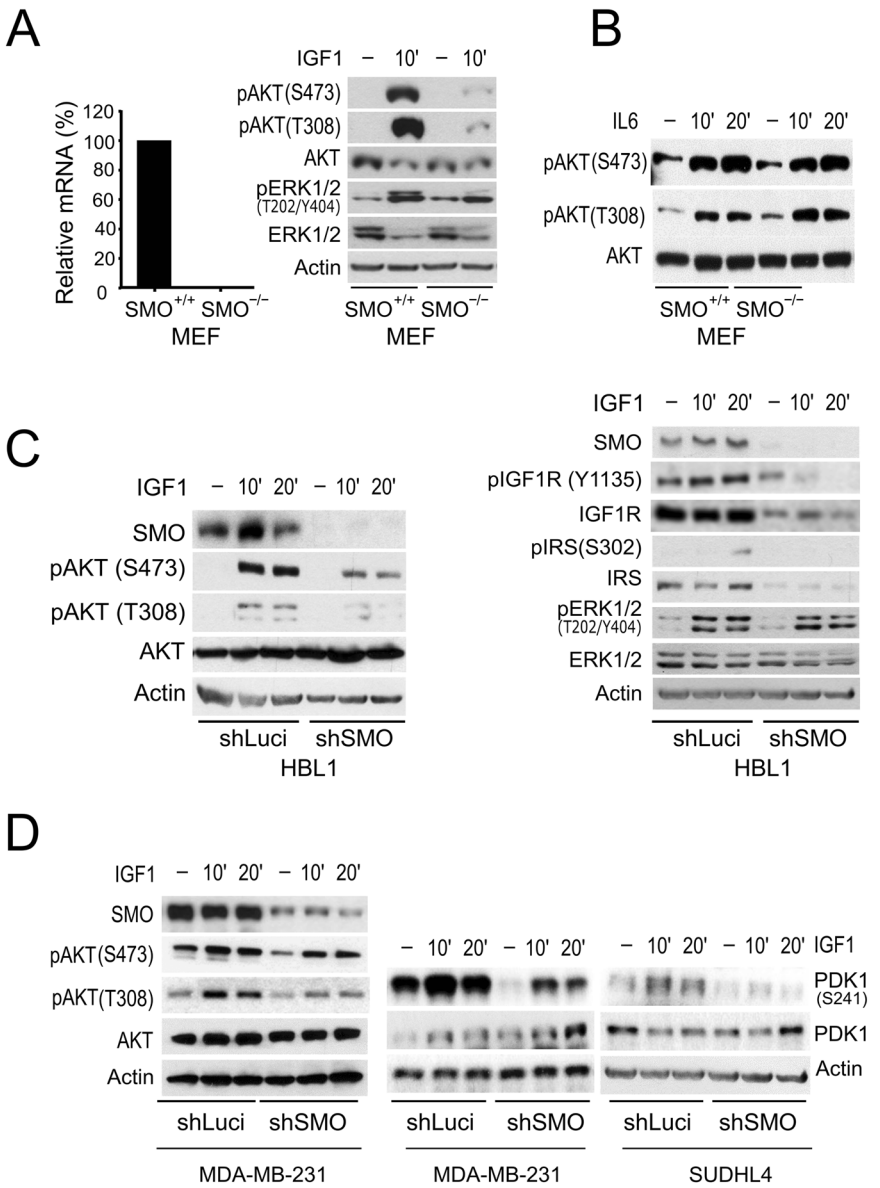

Fig. 2 SMO enhances IGF1R-mediated activation of AKT. All cells were cultured in the 2%-serum-containing medium for 18 h, and then stimulated with or without recombinant IGF1 (100 ng/ml) or interleukin 6 (IL6) (100 ng/ml) for the indicated time periods between 0-20 min. **A** $SMO^{-/-}$ MEF cells show a pronounced decrease in IGF1-stimulated phosphorylation of AKT but no significant suppression of ERK1/2 activation. **B** For comparison, the IL6-dependent activation of AKT is not impacted by the loss of SMO. **C** Knockdown of SMO (shSMO) in HBL1 DLBCL cells diminishes IGF1-stimulated activation of AKT phosphorylation, compared to a control knockdown of Luciferase (shLuci). The catalytic state of IGF1R was probed at Tyr1135 (1165) in the activation loop and displays a shift to very short-lived activation after SMO depletion while MAPK activation is not impacted. **D** AKT activation in MDA-MB-231 cells is also severely impacted by SMO depletion as is the activation of upstream PDK1 in both, MDA-MBA-231 breast cancer cells and the SUDHL4 DLBCL cell line.

downstream of IGF1R is insulin receptor substrate 1 (IRS1)-dependent and 3-phosphoinositide-dependent protein kinase (PDK1)-mediated. In line with the reduced activation of AKT, the phosphorylation of PDK1 at S241 is markedly abrogated in SMO-depleted MDA-MB-231 cells. We observed the same deficiency in PDK1 activation in SUDHL4 cells, a model system representing GC-type DLBCL. Altogether, our data suggest a significant impact of SMO on the IGF1R-mediated activation of AKT signaling that exists across multiple model systems.

SMO stabilizes IGF1R protein levels

In MEFs, MDA-MB-231, as well as in the DLBCL line HBL1, IGF1R levels strongly decreased after silencing or deleting *SMO* and increased after overexpression of recombinant hSMO (Fig. 3A). SMO may elevate the levels of IGF1R protein at the transcriptional level through canonical signaling by glioma-associated oncogene homolog (GLI) transcription factors. This final regulation at the *IGF1R* gene-level occurs predominantly through GLI2. The GLI1 transcription factor contributes to the initial response to SMO activation and the *GLI1* transcript is, in contrast to *GLI2*, itself subject to reinforcing regulation that is frequently used as a readout for canonical SMO signaling. Consistent with this SMO-dependent transcriptional feedback regulation of *GLI1*, transcript levels were reduced for *GLI1* in MDA-MB-231 shSMO knockdown cells while *IGF1R* transcript levels were not suppressed (Fig. 3B). In MEF SMO (−/−) cells, *GLI1* transcript levels are significantly reduced as expected. However, in contrast to the sensitivity of IGF1 signaling and IGF1R protein levels to SMO depletion, the

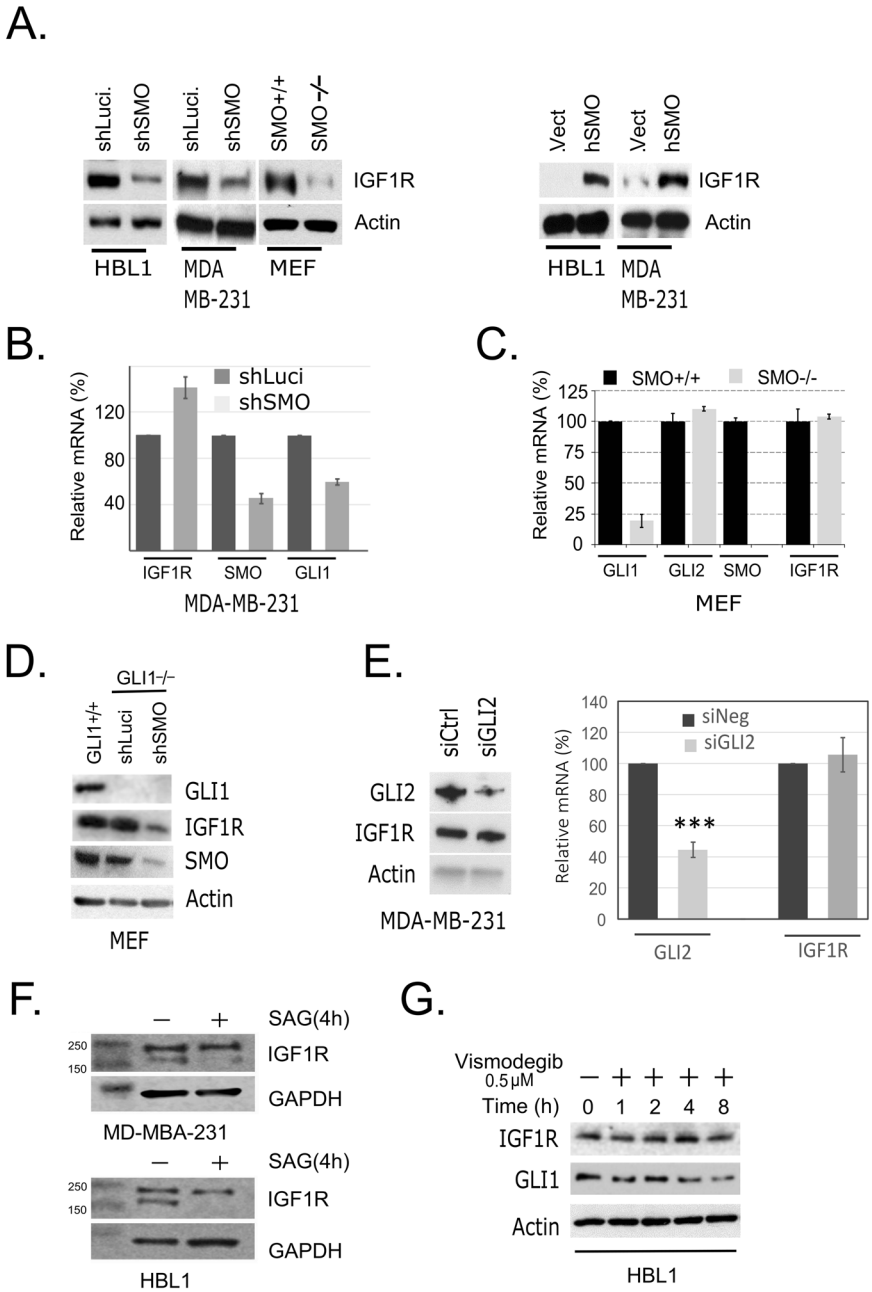

Fig. 3 SMO stabilizes IGF1R protein levels independent of canonical signaling. A Knockdown or absence of SMO in HBL1, MDA-MB-231, or MEF cells reduces the steady-state levels of IGF1R protein (left), while overexpression of recombinant human SMO (hSMO) results in a very pronounced increase of IGF1R (right). Note that the intensity range needed to show endogenous IGF1R (vector control) in panel (**B**) with an intensity that is comparable to the left panel would result in out-of-range signal for IGF1R in hSMO transfected cells. **B** Loss of SMO does not decrease mRNA levels of IGF1R. While the *Gli1* mRNA shows the expected regulatory response in the absence of SMO, the levels of *IGF1R* mRNA are not reduced in shSMO-treated MDA-MB-231 cells. **C** MEF(SMO$^{-/-}$) show reduced levels of *GLI* transcript, but not *IGF1R*. **D** The decrease in IGF1R protein levels after loss of SMO is a GLI1-independent response that occurs also in MEF(GLI1$^{-/-}$) cells. **E** The knockdown of *GLI2*, which is critical in canonical signaling, does not alter IGF1R protein levels. **F** In contrast to recombinant overexpression of SMO, activation of SMO by the small agonist SAG (1 μM) does not stabilize IGF1R. **G** Inhibition of SMO by Vismodegib does not reduce IGF1R levels. HBL1 cells were cultured in 10% serum-containing medium and then treated with or without Vismodegib (0.5 μM) for 0–8 h. Vismodegib activity is evident in the time-delayed decrease of GLI1 protein levels, reflecting the transcriptional feedback regulation of GLI1 by SMO.

levels of *IGF1R* mRNA were not altered (Fig. 3C). In addition, the sensitivity of IGF1R protein levels to a knockdown of SMO still occurred in MEF GLI1 (−/−) cells (Fig. 3D) and IGF1R levels were insensitive to the knockdown of GLI2 (Fig. 3E).

Data thus far point to a post-translational regulation of IGF1R levels, and the lack of impact of GLI1 or GLI2 depletion indicates a lack of involvement of canonical signaling in this regulation. To query this assumption more directly, we treated HBL1 cells with both, an SMO agonist and inhibitor. This treatment was carried out over a time interval that minimizes secondary transcriptional regulation, but allows for IGF1R turnover, the timing of which is analyzed more closely in Fig. 4. Activation of SMO by SAG, a small molecule agonist of SMO, did not increase the steady-state levels of IGF1R (Fig. 3F). Likewise, treatment of HBL1 cells with

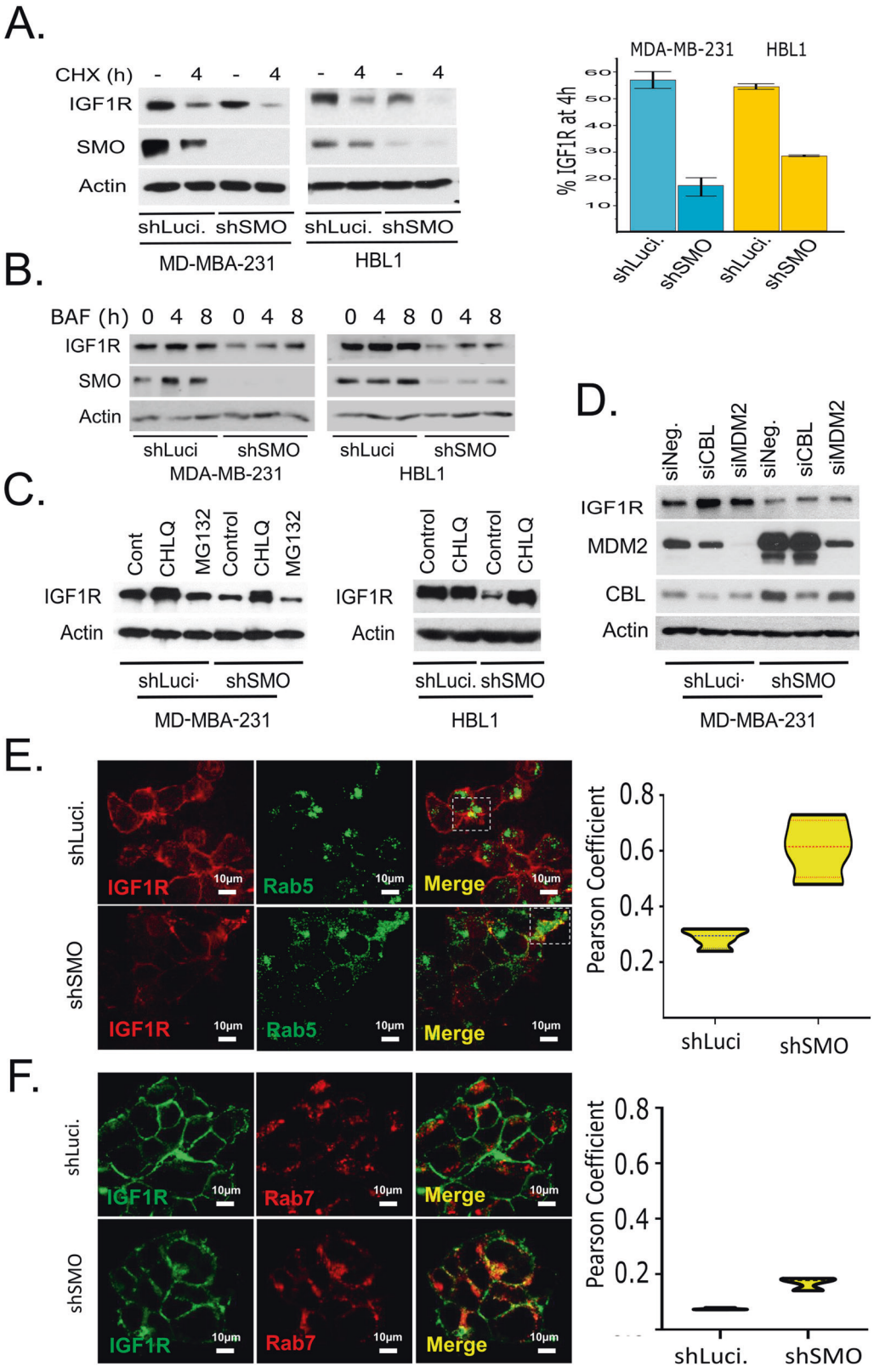

Vismodegib, a clinically approved inhibitor of SMO that inhibits canonical signaling, did not alter the levels of IGF1R (Fig. 3G). Over the same time period, GLI1 levels showed the time-delayed decrease that would be expected for the inhibition of canonical signaling by SMO.

Consistent with a model of regulation through protein stability, the loss of SMO results in a pronounced decrease in IGF1R receptor half-life, measured after 4 h of treatment with cycloheximide (Fig. 4A). The extent to which the receptor half-life was decreased in MDA-MB-231 versus HBL1 cells is consistent with the

Fig. 4 Loss of SMO redirects IGF1R to late endosomes and lysosomal degradation. A MDA-MB-231 and HBL1 cells were cultured in 10% serum medium and then treated with or without cycloheximide (CHX) for 4 h. In the absence of SMO, the half-life of IGF1R is reduced in both MDA-MB-231 and HBl1 cells. Quantification of IGF1R levels was carried out at 4 h from experimental triplicates after cycloheximide treatment. **B** In shSMO cells, inhibition of lysosomal activity with Bafilomycin A for the indicated times results in a rapid rebound of IGF1R from low starting levels. MDA-MB-231 and HBL1 cells were cultured in 10% serum medium and then treated with or without Bafilomycin A (BAF, 100 nM) for 0–8 h. **C** Treatment with chloroquine (50 μM), for 4 h, but not the proteasome inhibitor MG132 (10 μM), results in a pronounced recovery of IGF1R. **D** While CBL and MDM2 are upregulated in SMO-depleted cells, their knockdown does not reverse the decrease in IGF1R. **E** In MDA-MB-231 cells, the colocalization of IGF1R and the early endosome marker RAB5 shows a small but not statistically significant increase after depletion of SMO. **F** By contrast, the colocalization of IGF1R and the late endosome marker RAB7 is significantly increased.

impact on total levels observed earlier after SMO knockdown (Fig. 3A). In order to test whether the reduced IGF1R protein half-life was due to increased lysosomal degradation, we inhibited lysosomal function with Bafilomycin A1, a direct inhibitor of the V-type proton ATPase (V-ATPase)[36] (Fig. 4B). IGF1R levels showed significant recovery from low starting levels. This increase may be an underestimate since BAF can negatively impact system-wide processing. When the lysosomal activity was instead inhibited with chloroquine, an increase of IGF1R levels was also apparent in the controls (as expected), but the relative increase was far more pronounced in shSMO-treated cells (Fig. 4C). By contrast, treatment with the proteasomal inhibitor MG132 did not result in a recovery of IGF1R levels.

The degradation and turnover of IGF1R is subject to regulation through ubiquitination. Both, casitas B-lineage lymphoma proto-oncogene (CBL) and mouse double minute 2 (MDM2) are central in this regulation. Indeed, knockdown of either E3-ligase results in a small but noticeable increase in the steady-state levels of IGF1R in control cells, despite the low efficiency of CBL knockdown in this setting (Fig. 4D). Both E3-ligases were efficiently knocked down in shSMO-treated cells, but without recovery of the reduced IGF1R levels in SMO-depleted cells. While this evaluation does not exclude the involvement of other E3-ligases, it indicates that the loss of IGF1R protein levels is likely not the consequence of increases in ubiquitination upon loss of SMO.

The above data suggest that after SMO depletion, IGF1R could be routed to different endosomal compartments. To further validate this prediction, we evaluated the impact of SMO knockdown on the colocalization of IGF1R with RAS-associated proteins RAB5 and RAB7, established markers of the early and late endosomal compartments, respectively. Depletion of SMO in MDA-MB-231 results in a modest shift of IGF1R to the early endosomal compartment marked by RAB5 (Fig. 4E) that does not reach statistical significance. Once in the early endosome, membrane proteins are sorted and transported to late endosomes and lysosomes for degradation or are routed for recycling. We next investigated the localization of IGF1R and the late endosome marker RAB7. The colocalization of IGF1R and RAB7 markedly increased after SMO knockdown (Fig. 4F). Consistent with the results of lysosomal inhibitors, this indicates that loss of SMO redirects more IGF1R from the early endosomal compartment towards lysosomal degradation.

SMO localizes to raft microdomains and regulates the levels of raft-associated IGF1R and activated AKT

Signaling through the PTEN/AKT pathway requires AKT to be localized to raft microdomains where relevant signaling components are congregated[37,38]. Lipid rafts are segments of the plasma membrane that are highly dynamic and composed mainly of saturated phospholipids, cholesterol, and glycosphingolipids such as gangliosides (e.g., GM1)[39]. IGF1R in its resting state resides primarily in raft microdomains. Activated receptors can internalize directly from rafts via caveolae, or receptors can exit rafts to endocytose via clathrin-mediated endocytosis. In both cases, signaling continues during the endocytosis process, but the routing changes the nature of interacting partners. Since studies in *Drosophila* suggest a raft localization of SMO, we evaluated whether this was also true for human SMO. We first analyzed the colocalization of endogenous SMO and CD59 on the cell surface of HBl1 cells (Fig. 5A). As a glucosyl-phosphatidyl-inositol anchored protein, CD59 localizes to lipid rafts[40]. When live HBL1 lymphoma cells were treated with CD59 primary and associated secondary antibody to cluster and visualize rafts, subsequent antibody staining for endogenous SMO revealed a high degree of colocalization. Transferrin receptor (TF-R) is not localized in rafts. By contrast to SMO, a directed antibody and fluorescently labeled secondary antibody does generate clusters of TF-R under the same conditions, and the overlap with SMO is minimal (Fig. 5B).

As an additional means of validation, we transfected MDA-MB-231 cells with a SMO-mCherry fusion protein and clustered raft microdomains with fluorescently labeled cholera toxin subunit B (CTB). Heptameric CTB clusters rafts by virtue of its binding to the raft constituent ganglioside GM1. Under these conditions, SMO-mCherry and CTB show a strong colocalization (Fig. 5C). To evaluate the link to IGF1R localization and AKT activation, we subjected untransfected MDA-MB-231 cells to a detergent-free sucrose gradient membrane fractionation. We observed the presence of endogenous SMO in the raft fractions marked by caveolin and flotillin[41], but not in the non-raft fraction of the membrane (marked by TF-R), or cytoplasmic fraction (marked by Erk1/2) (Fig. 5D). While the portion of the total AKT that is membrane localized is small, this pool is crucial for IGF1R signaling through phosphatidylinositol 3-phosphate (PI3P) and PI3K. We, therefore, carried out a fractionation in shLuci control and shSMO MDA-MB-231 cells and focused the analysis of the protein distribution on the different membrane compartments (fractions 1–7) (Fig. 5E). SMO and the majority of IGF1R localizes to the lipid raft fraction in the shLuci control. While the bulk of AKT and pAKT is not raft localized, the raft fractions in shLuci control cells contain a significant amount of pAKT and the distribution is consistent with that seen for the membrane fractions in Fig. 5D. For shSMO-treated cells, the loss of SMO results in a pronounced drop in raft-localized IGF1R receptor levels and in a redistribution of AKT. Overall levels of AKT are markedly reduced in the raft fraction, consistent with our previously reported role of SMO/ubiquitin-specific peptidase 8 (USP8)/TRAF6 dependent remodeling of AKT ubiquitination from lysine 48 branched K48-Ub to K63-Ub modification of AKT, a modification change that has been associated with both stabilization and membrane recruitment[34]. Interestingly, the remaining low levels of raft-associated AKT have almost entirely lost 3-phosphoinositide-dependent protein kinase (PDK1)-dependent phosphorylation in their activation loop at T308, while the phosphorylation of the remaining AKT in the hydrophobic motif, carried out by the mechanistic target of rapamycin kinase complex 2 (mTORC2), is reduced to a far lesser extent. The strong correlation between the drop in total AKT and pAKT(T308) indicates that the majority of raft-localized AKT is localized to this compartment in a PI3P signaling-dependent manner. This fraction of AKT that generates a highly oncogenic signal and is crucial for IGF1R signal transduction is almost entirely lost upon knockdown of SMO, and raft localized IGF1R is markedly depleted.

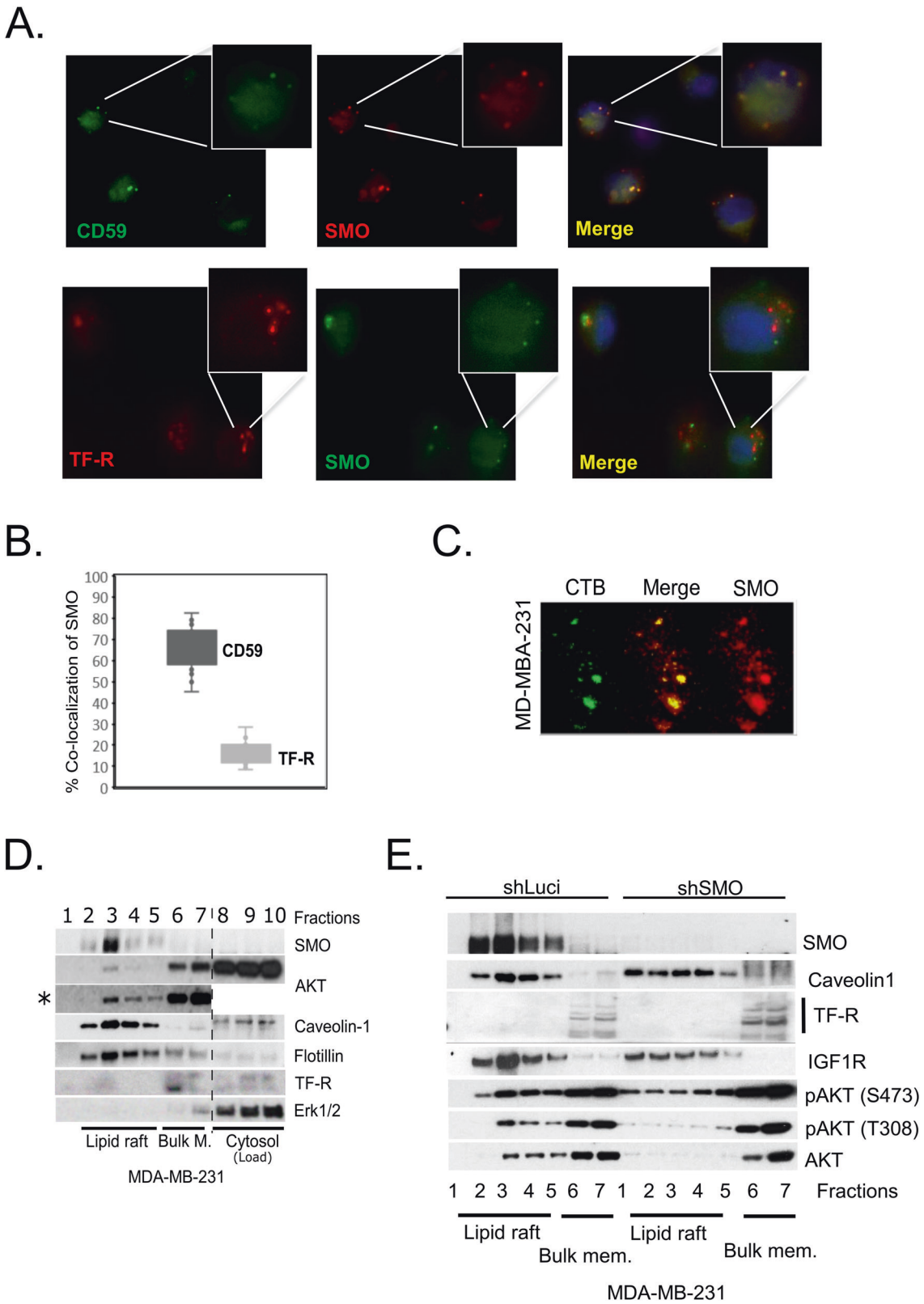

Fig. 5 SMO localizes to raft microdomains and stabilizes IGF1R and pAKT levels in this compartment. A Immunohistochemistry and colocalization analysis of the raft marker CD59 or transferrin receptor (TF-R) as the bulk membrane control with SMO in HBL1 cells. **B** Quantification of data in panel (**A**) shows that SMO colocalizes with CD59 but not with TF-R. **C** Clustering of SMO-Cherry fusion protein in MDA-MB-231 with heptameric and fluorescently labeled cholera toxin subunit B (CTB). **D** Detergent-free fractionation of MDA-MB-231 cells places endogenous SMO in the raft fraction. Caveolin and Flotillin mark the raft fraction, TF-R the bulk membrane fraction, and ERK1/2 the cytosol. **E** Membrane fractions (1–7) in the presence or absence of SMO. The loss of SMO results in a reduction of IGF1R and very pronounced loss of AKT in the raft fraction. The loss of AKT coincides with an all but complete loss of pAKT(T308), the target of PDK1, while the small portion of AKT that is phosphorylated at S473 (mThor) is largely unaffected.

DISCUSSION

Aberrant activation of the PI3K/AKT signaling pathway is crucial in many aspects of cancer cell proliferation and survival, and upstream receptors are a significant source of AKT activation. We previously demonstrated that SMO can increase the levels of activated and membrane-localized AKT through stabilization of both AKT and pAKT, independent of the nature of the AKT activating event[34]. We now show that IGF1R-mediated activation of AKT is enhanced by SMO and is markedly diminished upon SMO depletion. This novel mode of AKT signal enhancement by SMO is mediated through an increase in the steady-state levels of IGF1R as well as an optimization of the IGF1R signaling context that favors AKT activation. This change is most pronounced for the phosphorylation of AKT in its activation loop, which occurs in a PI3P-dependent manner and is known to be the primary predictor for an aggressive cancer phenotype. This link between SMO, IGF1R, and the levels of membrane-localized pAKT signaling is also reflected by the significant positive correlation between SMO expression in primary tumors and disease outcomes. This is also consistent with a previous study demonstrating that SMO expression is an independent marker for colon and breast cancer progression[42,43].

Oncogenic effects of Hh pathway components are generally thought to be mediated by elevated transcriptional activation of GLI1 target genes through canonical Hh signaling, which in turn can be enhanced by elevated ligand levels, activating mutations of SMO, or inactivating mutations/loss of PTCH1[13]. Recent studies have shown that signaling through growth factor receptors, such as IGF1R, enhances the constitutive transcriptional activation of *GLI1* by Hh ligands[25] while IGF-2 is a transcriptional target of *GLI*[44]. However, in these scenarios, SMO acts as a classic signal transducer of transcription-centered regulation. Existing treatment modalities are therefore aimed at and optimized for maximum disruption of canonical signaling.

Our current study introduces a new level of connectivity between SMO and IGF1R-mediated activation of AKT that is post-translational in nature and acts at the level of receptor stabilization and localization. In addition, this mode of regulation is independent of canonical signaling. For IGF1R, we show that lower receptor levels are the consequence of a shorter protein half-life, resulting in lower receptor numbers and significantly diminished signaling through AKT. Further analysis shows that the loss of SMO impacts the extent to which IGF1R is directed toward the lysosome for degradation.

The remaining pool of IGF1R is markedly shifted in its localization. This introduces both a quantitative and qualitative impact of SMO on IGF1R-mediated signaling. In the case of IGF1R, β-arrestin aided internalization of IGF1R through clathrin-mediated endocytosis correlates with strong activation of the MAPK pathway[6]. Activation of the MAPK pathway is generally very temporal in nature with maximum MAPK phosphorylation frequently at 30 min or less post stimulation. The time required for IGF1R to remain in the catalytically active state is well below 10 min[10,45]. This signaling mode would not be impacted by a loss of IGF1R in the raft compartment, and rapid internalization to acidified compartments would be consistent with ligand dissociation and an early cessation of activation loop phosphorylation. Whether the rapid loss of activation loop phosphorylation upon ligand stimulation and continued MAPK activation in SMO-depleted cells is indeed associated with this pathway requires further study. The dominant impact of SMO depletion occurs in the raft-localized PI3K/AKT signaling pathway. This pathway is impacted both by the loss in receptor numbers and the non-favorable signaling context of the remaining receptors. This impact on IGF1R-mediated AKT activation would be further compounded by the loss of previously reported and SMO-mediated stabilization of activated AKT that is independent of the initial source of AKT activation[34].

The extent to which these additional modes of action, beyond canonical signaling, may utilize parts of the established signal transduction machinery for SMO or alternatively rely exclusively on scaffold functions, remains to be seen. The current data suggest that a study of these novel capabilities of SMO may have therapeutic potential. It further suggests that the inhibition of canonical signaling should not be the only and may not be the best readout used for the development of new SMO inhibitors, especially in cancer settings with a pronounced PI3K/AKT signaling contribution.

DATA AVAILABILITY

The datasets used and/or analyzed during this study are available from the corresponding author on reasonable request.

REFERENCES

1. Pollak, M. The insulin and insulin-like growth factor receptor family in neoplasia: an update. *Nat. Rev. Cancer* **12**, 159–169 (2012).
2. Jerome, L., Shiry, L. & Leyland-Jones, B. Deregulation of the IGF axis in cancer: epidemiological evidence and potential therapeutic interventions. *Endocr. Relat. Cancer* **10**, 561–578 (2003).
3. Hua, H., Kong, Q., Yin, J., Zhang, J. & Jiang, Y. Insulin-like growth factor receptor signaling in tumorigenesis and drug resistance: a challenge for cancer therapy. *J. Hematol. Oncol.* **13**, 64 (2020).
4. Crudden, C. et al. Blurring boundaries: receptor tyrosine kinases as functional G protein-coupled receptors. *Int. Rev. Cell Mol. Biol.* **339**, 1–40 (2018).
5. Vecchione, A., Marchese, A., Henry, P., Rotin, D. & Morrione, A. The Grb10/Nedd4 complex regulates ligand-induced ubiquitination and stability of the insulin-like growth factor I receptor. *Mol. Cell. Biol.* **23**, 3363–3372 (2003).
6. Girnita, L. et al. Beta-arrestin and Mdm2 mediate IGF-1 receptor-stimulated ERK activation and cell cycle progression. *J. Biol. Chem.* **282**, 11329–11338 (2007).
7. Lin, Y. et al. SUMO-modified insulin-like growth factor 1 receptor (IGF-1R) increases cell cycle progression and cell proliferation. *J. Cell. Physiol.* **232**, 2722–2730 (2017).
8. Aleksic, T. et al. Type 1 insulin-like growth factor receptor translocates to the nucleus of human tumor cells. *Cancer Res.* **70**, 6412–6419 (2010).
9. Chughtai, S. The nuclear translocation of insulin-like growth factor receptor and its significance in cancer cell survival. *Cell Biochem. Funct.* **38**, 347–351 (2020).
10. Sehat, B., Andersson, S., Vasilcanu, R., Girnita, L. & Larsson, O. Role of ubiquitination in IGF-1 receptor signaling and degradation. *PLoS ONE* **2**, e340 (2007).
11. Crudden, C. et al. Below the surface: IGF-1R therapeutic targeting and its endocytic journey. *Cells* **8**, 1223 (2019).
12. Riobo, N. A., Saucy, B., Dilizio, C. & Manning, D. R. Activation of heterotrimeric G proteins by Smoothened. *Proc. Natl Acad. Sci. USA* **103**, 12607–12612 (2006).
13. Xie, J. et al. Activating Smoothened mutations in sporadic basal-cell carcinoma. *Nature* **391**, 90–92 (1998).
14. Byrne, E. F. et al. Structural basis of Smoothened regulation by its extracellular domains. *Nature* https://doi.org/10.1038/nature18934 (2016).
15. Goetz, S. C. & Anderson, K. V. The primary cilium: a signalling centre during vertebrate development. *Nat. Rev. Genet.* **11**, 331–344 (2010).
16. Eggenschwiler, J. T. & Anderson, K. V. Cilia and developmental signaling. *Annu. Rev Cell. Dev. Biol.* **23**, 345–373 (2007).
17. Kuzhandaivel, A., Schultz, S. W., Alkhori, L. & Alenius, M. Cilia-mediated hedgehog signaling in Drosophila. *Cell. Rep.* **7**, 672–680 (2014).
18. Shi, D. et al. Smoothened oligomerization/higher order clustering in lipid rafts is essential for high Hedgehog activity transduction. *J. Biol. Chem.* **288**, 12605–12614 (2013).
19. Myers, B. R., Neahring, L., Zhang, Y., Roberts, K. J. & Beachy, P. A. Rapid, direct activity assays for Smoothened reveal Hedgehog pathway regulation by membrane cholesterol and extracellular sodium. *Proc. Natl Acad. Sci. USA* **114**, E11141–E11150 (2017).
20. Uddin, S. et al. Role of phosphatidylinositol 3′-kinase/AKT pathway in diffuse large B-cell lymphoma survival. *Blood* **108**, 4178–4186 (2006).
21. Pfeifer, M. et al. PTEN loss defines a PI3K/AKT pathway-dependent germinal center subtype of diffuse large B-cell lymphoma. *Proc. Natl Acad. Sci. USA* **110**, 12420–12425 (2013).
22. Abubaker, J. et al. PIK3CA mutations are mutually exclusive with PTEN loss in diffuse large B-cell lymphoma. *Leukemia* **21**, 2368–2370 (2007).
23. Renne, C. et al. High expression of several tyrosine kinases and activation of the PI3K/AKT pathway in mediastinal large B cell lymphoma reveals further similarities to Hodgkin lymphoma. *Leukemia* **21**, 780–787 (2007).

24. Chen, L. et al. SYK inhibition modulates distinct PI3K/AKT- dependent survival pathways and cholesterol biosynthesis in diffuse large B cell lymphomas. *Cancer Cell* **23**, 826–838 (2013).
25. Riobo, N. A., Lu, K., Ai, X., Haines, G. M. & Emerson, C. P. Jr. Phosphoinositide 3-kinase and Akt are essential for Sonic Hedgehog signaling. *Proc. Natl Acad. Sci. USA* **103**, 4505–4510 (2006).
26. Pirskanen, A., Kiefer, J. C. & Hauschka, S. D. IGFs, insulin, Shh, bFGF, and TGF-beta1 interact synergistically to promote somite myogenesis in vitro. *Dev. Biol.* **224**, 189–203 (2000).
27. Madhala-Levy, D., Williams, V. C., Hughes, S. M., Reshef, R. & Halevy, O. Cooperation between Shh and IGF-I in promoting myogenic proliferation and differentiation via the MAPK/ERK and PI3K/Akt pathways requires Smo activity. *J. Cell. Physiol.* **227**, 1455–1464 (2012).
28. Hans, C. P. et al. Confirmation of the molecular classification of diffuse large B-cell lymphoma by immunohistochemistry using a tissue microarray. *Blood* **103**, 275–282 (2004).
29. Kim, J. E. et al. Sonic hedgehog signaling proteins and ATP-binding cassette G2 are aberrantly expressed in diffuse large B-cell lymphoma. *Mod. Pathol.* **22**, 1312–1320 (2009).
30. Agarwal, N. K., Qu, C., Kunkalla, K., Liu, Y. & Vega, F. Transcriptional regulation of serine/threonine protein kinase (AKT) genes by glioma-associated oncogene homolog 1. *J. Biol. Chem.* **288**, 15390–15401 (2013).
31. Blank, N. et al. Cholera toxin binds to lipid rafts but has a limited specificity for ganglioside GM1. *Immunol. Cell. Biol.* **85**, 378–382 (2007).
32. Prior, I. A. et al. GTP-dependent segregation of H-ras from lipid rafts is required for biological activity. *Nat. Cell Biol.* **3**, 368–375 (2001).
33. Singh, R. R. et al. ABCG2 is a direct transcriptional target of hedgehog signaling and involved in stroma-induced drug tolerance in diffuse large B-cell lymphoma. *Oncogene* **30**, 4874–4886 (2011).
34. Qu, C. et al. Smoothened stabilizes and protects TRAF6 from degradation: a novel non-canonical role of smoothened with implications in lymphoma biology. *Cancer Lett.* **436**, 149–158 (2018).
35. Stromberg, T. et al. Picropodophyllin inhibits proliferation and survival of diffuse large B-cell lymphoma cells. *Med. Oncol.* **32**, 188 (2015).
36. Drose, S. & Altendorf, K. Bafilomycins and concanamycins as inhibitors of V-ATPases and P-ATPases. *J. Exp. Biol.* **200**, 1–8 (1997).
37. Liu, P., Cheng, H., Roberts, T. M. & Zhao, J. J. Targeting the phosphoinositide 3-kinase pathway in cancer. *Nat. Rev. Drug Discov.* **8**, 627–644 (2009).
38. Calay, D. et al. Inhibition of Akt signaling by exclusion from lipid rafts in normal and transformed epidermal keratinocytes. *J. Investig. Dermatol.* **130**, 1136–1145 (2010).
39. Reed, R. A., Mattai, J. & Shipley, G. G. Interaction of cholera toxin with ganglioside GM1 receptors in supported lipid monolayers. *Biochemistry* **26**, 824–832 (1987).
40. Kimberley, F. C., Sivasankar, B. & Paul Morgan, B. Alternative roles for CD59. *Mol. Immunol.* **44**, 73–81 (2007).
41. Morrow, I. C. et al. Flotillin-1/reggie-2 traffics to surface raft domains via a novel Golgi-independent pathway. Identification of a novel membrane targeting domain and a role for palmitoylation. *J. Biol. Chem.* **277**, 48834–48841 (2002).
42. Ding, Y. L., Wang, Q. S., Zhao, W. M. & Xiang, L. Expression of smoothened protein in colon cancer and its prognostic value for postoperative liver metastasis. *Asian Pac. J. Cancer Prev.* **13**, 4001–4005 (2012).
43. Tao, Y., Mao, J., Zhang, Q. & Li, L. Overexpression of Hedgehog signaling molecules and its involvement in triple-negative breast cancer. *Oncol. Lett.* **2**, 995–1001 (2011).
44. Ingram, W. J., Wicking, C. A., Grimmond, S. M., Forrest, A. R. & Wainwright, B. J. Novel genes regulated by Sonic Hedgehog in pluripotent mesenchymal cells. *Oncogene* **21**, 8196–8205 (2002).
45. Li, W. & Miller, W. T. Role of the activation loop tyrosines in regulation of the insulin-like growth factor I receptor-tyrosine kinase. *J. Biol. Chem.* **281**, 23785–23791 (2006).

ACKNOWLEDGEMENTS

We thank Dr. James K. Chen (Department of Chemical and Systems Biology, Stanford University School of Medicine) for providing the *SMO*$^{-/-}$ (MEF) cells. We also thank Dr. Amit Deepak Amin for helpful comments for the manuscript. We acknowledge the University of Miami/Sylvester Comprehensive Cancer Center Histology Core and the Biorepository and Tissue Procurement Facility. This work has been supported by research funds from National Cancer Institute, National Institute of Health (grant R01CA222918) (to R.L. and F.V.), Sylvester Comprehensive Cancer Center/University of Miami (to R.L. and F.V.), the American Society of Hematology (ASH) bridge award (to F.V.) and Woman Cancer Association of Florida (to R.L.).

AUTHOR CONTRIBUTIONS

Conception and design: N.K.A., R.L. and F.V. Development of methodology: N.K.A., R.L. and F.V. Acquisition of the data: N.K.A., C.H.K., K.K., A.V., S.S., S.M., R.L. and F.V. Analysis and interpretation of the data (e.g., statistical analysis, biostatistics, computational analysis): N.K.A., R.L. and F.V. Writing, review, and/or revision of the manuscript: N.K.A., D.B., F.V. and R.L. Administrative, technical, or material support (i.e., reporting or organizing data, constructing databases): N.K.A., R.L. and F.V. Study supervision: R.L. and F.V.

COMPETING INTERESTS

The authors declare no competing interests.

ETHICS APPROVAL AND CONSENT TO PARTICIPATE

Tissue specimens were collected from Sylvester Comprehensive Cancer Center, University of Miami under the approved institutional review board committee. The study was conducted in accordance with the declaration of Helsinki.

ADDITIONAL INFORMATION

Supplementary information The online version contains supplementary material available at https://doi.org/10.1038/s41374-021-00702-6.

Correspondence and requests for materials should be addressed to Francisco Vega or Ralf Landgraf.

Reprints and permission information is available at http://www.nature.com/reprints

Publisher's note Springer Nature remains neutral with regard to jurisdictional claims in published maps and institutional affiliations.